P2.52 COMBINING SATELLITE DATA, TRAJECTORY MODELING AND SURFACE INSOLATION MEASUREMENTS TO DEDUCE THE DIRECT RADIATIVE EFFECT OF SMOKE AEROSOL

Paul W. Stackhouse Jr.[1], R. Bradley Pierce[1], Bryan A. Baum[1], and Roberta C. DiPasquale[2]

[1]Atmospheric Sciences Division,NASA Langley Research Center, Hampton, Virginia 23681-0001

[2]Analytical Services and Materials, Inc., Hampton, VA, 23666

1. INTRODUCTION

The need to develop a climatology of aerosols and their direct radiative forcing has been identified as a critical gap in our knowledge of the earth's atmosphere and may play a large role in the process of climate change. Recognizing this need, the Global Aerosol Climatology Project (GACP) was instituted by NASA and under the auspices of the World Climate Research Programme (WCRP)/ Global Energy and Water Cycle Experiment (GEWEX).

One problem hampering the development of satellite based aerosol climatology is that retrievals depend upon *a priori* assumptions regarding the aerosol size distribution and/or composition. However, smoke aerosols are much more absorptive than the aerosols assumed in such algorithms. Therefore, analysis methods that develop statistics regarding the possible distributions of aerosol types would improve satellite retrievals of aerosol optical properties. Large smoke plumes from biomass burning events are among the aerosol producing events that also greatly affect the solar insolation, sometimes for long periods. One such event occurred during the summer of 1989, when a large outbreak of boreal forest fires occurred in Manitoba Canada. These fires were so large that several large areas had to be evacuated and there was evidence of smoke aerosols as far south as Florida and across the Atlantic.

The purpose of this paper is to demonstrate one possible means of deriving distributions of biomass burning aerosols resulting from boreal forrest fires by combining satellite observations from AVHRR and trajectory modeling using the NASA Langley Trajectory Model (LTM). Surface radiometric measurements serve as a first order validation of the technique and are used to estimate the radiative effect of the smoke on the solar insolation.

**Corresponding author address:* Paul W. Stackhouse, Jr., NASA Langley Research Center, MS 420, Hampton, VA, 23681; e-mail: p.w.stackhouse@larc.nasa.gov

2. THE FOREST FIRES OF 1989 IN MANITOBA, CANADA

The 1989 Manitoba fire season set a record for the number of fires and the area burned in Manitoba. According to the Canadian Northern Forestry Centre, the period from July 21 through July 23, 1989 was considered to be the most critical in terms of wide spread burning (Hirsch 1991). The fire outbreaks were so severe that a number of communities in northern Manitoba were evacuated between July 19 and July 26, 1989 (Hirsch 1991). Hirsch also reported that wind speeds associated with a ridge system averaged between 20-33 km/h with gusts over 50 km/h at some stations increasing both the intensity and spreading of the fires. Figure 1a provides an image of the fire area from AVHRR Local Area Coverage (1 km resolution in the visible channels) and indicates several areas evacuated due to the smoke and fire.

3. FIRE/SMOKE IDENTIFICATION USING AVHRR

The scene identification algorithm of Baum and Trepte (1999) is used to analyze radiances from AVHRR Local Area Coverage data (at 1 km resolution) and identify areas likely to be sources of smoke aerosol. This method works by applying a set of daytime spectral channel tests using the radiances from all five of the AVHRR standard channels at center wavelengths of 0.63 μm, 0.86 μm, 3.7 μm, 11 μm, and 12 μm. The tests are applied on a pixel-by-pixel basis to discriminate between clouds, sunglint, snow, smoke, and fires using measured reflectance, reflectance ratios, brightness temperatures, and brightness temperature differences to those quantities observed and/ or expected in a clear-sky. The threshold ranges for the various spectral tests are based upon previous studies (e.g., Kaufman *et. al.*, 1990), radiative transfer calculations and extensive operational testing. This algorithm is currently limited to forest

surfaces due to the difficulty of obtaining smoke and fire detection over bright, variable, and hot surfaces (e.g., Matson *et al.* 1987). We define the minimum reflectance thresholds to give at least a 4-5% increase over the background forest and ocean reflectance.

Figure 1b shows the results from the smoke/fire/cloud mask algorithm as described above for the AHVRR LAC image in figure 1a. Frontal clouds are the brightest structures present in Fig 1a and extend roughly from the northeast corner (near the Hudson Bay) to the southwest corner of the image. Figure 1b identifies these features as clouds. The numbers 1 - 4 in Fig. 1a are located just above patches of light gray areas that are narrow to the west and widen to the east corresponding to the downwind direction. These are classic smoke plume structures and these areas are identified as such by the algorithm as shown in Fig. 1b. At the origin of these plume structures are located clusters pixels identified as fires. These fire pixels are later used to initialize the trajectory calculations. Based on further analysis it was determined that Fig. 1b provides a consistent and physical representation of the fire scene in Fig. 1a.

4. TRAJECTORY MODELING

Satellite pixels identified as containing surface fires are assumed to act as a source of smoke aerosols. These smoke aerosols are then assumed to be contained within boundary layer air parcels over fire locations. The NASA Langley Trajectory Model (LTM) is used to predict the 3D displacement of the smoke containing air parcels. The trajectory model has been used in conjunction with photochemical models and satellite observations to study transport and photochemical processes in the lower and middle stratosphere using operational analyses from a wide range of forecasting centers (e.g., Pierce *et al.* 1997; Fairlie *et al.* 1997). The LTM uses a fourth-order Runge-Kutta scheme within an isentropic framework using winds, temperatures, relative humidity, and diabatic heating rates from operational analyses. To treat the problem of smoke aerosols in the troposphere, the fall out rates of the smoke aerosol are treated as coarse scavenging. In this case, LTM is initialized using the meteorological fields from the European Centre for Medium-Range Weather Forecasts analysis.

The LTM is used to trace smoke containing air parcels from fire regions over a period of 10 days in

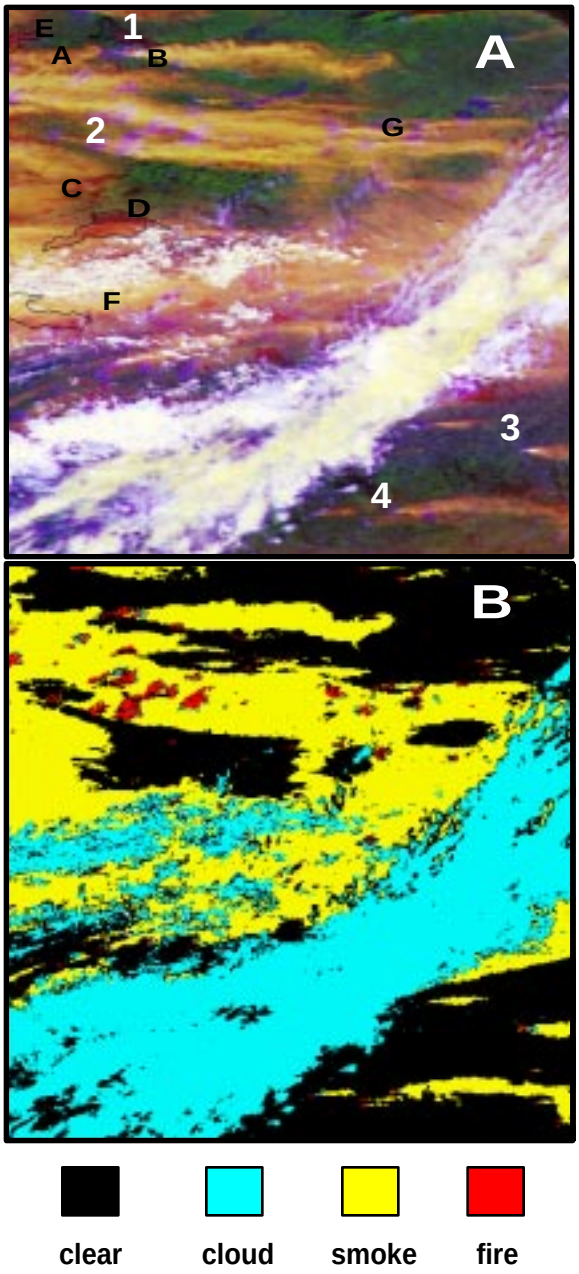

Figure 1: The top panel (A) is a NOAA-11 AVHRR image from 23, July, 1989 over northern Manitoba, Canada. The small black letters in this figure correspond to locations evacuated due to the excessive smoke and fire. The bottom panel (B) gives the results of a cloud mask/smoke/fire mask (Baum and Trepte, 1999).

a global context. From the analysis, given a particular grid box (which we have taken as 1 degree equal angle here) the total number of aerosol containing parcels and the relative concentration of those aerosols are computed. As a first approach, we queried grid boxes containing surface radiome-

ter sites in Canada and the United States for the smoke aerosol information. We then correlate the predicted arrival and intensity of smoke to that location with the time series of surface radiometric measurements. A sampling of the preliminary results are shown below.

5. SURFACE OBSERVATIONS

For the purposes of illustration, the results of the satellite analysis and LTM are shown with radiometric observations and predictions for Madison, Wisconsin and St. Pierre and Miquelon (an island located just south of the island of New Foundland, Canada) are shown in Figs. 2 and 3 respectively. Both figures show the time series of clouds, smoke aerosols and radiation for the period of July 22-31 as initialized by the fires that occurred on July 23. The top panel in each figure gives the 6-hourly cloud fraction as predicted by the ECMWF Reanalyses (ERA-15). The center panel gives the time series of the mean fraction of initial burden of the smoke aerosols (referred to as “C-burden” although the actual mass of carbon has not yet been estimated). The bottom panel of each figure gives the time series of the daily averaged solar insolation (W m^{-2}) from observations and the ERA-15 analysis. For both locations, the predicted arrival of the smoke aerosol corresponded to a prediction of little or no cloud by the ERA-15 analysis. Since the reanalysis has no information regarding smoke aerosols, the differences between the predicted ERA-15 and observed daily averaged fluxes are evidence of the radiative forcing of the smoke aerosols for those particular days.

In Fig. 2, day 210 corresponded to the day for which the maximum amount of smoke aerosols were predicted. The difference between the daily averaged solar insolation between the ERA-15 and the observations was 80 W m^{-2}. On the subsequent day the difference exceeded 130 W m^{-2}. Interestingly, the ERA-15 and observed daily averaged fluxes agreed to within 20 W m^{-2} for the seven days prior to day 210 for a variety of cloud conditions. Thus, the differences on day 210 and 211 are significantly higher, possibly indicating the direct radiative effect of the smoke. Similarly for Fig 3., days 206 to 211 were predicted to be days when smoke aerosol advected over the site. During this period of time the differences between ERA-15 and observed daily averaged solar insolation are between 80 and 100 W m^{-2}.

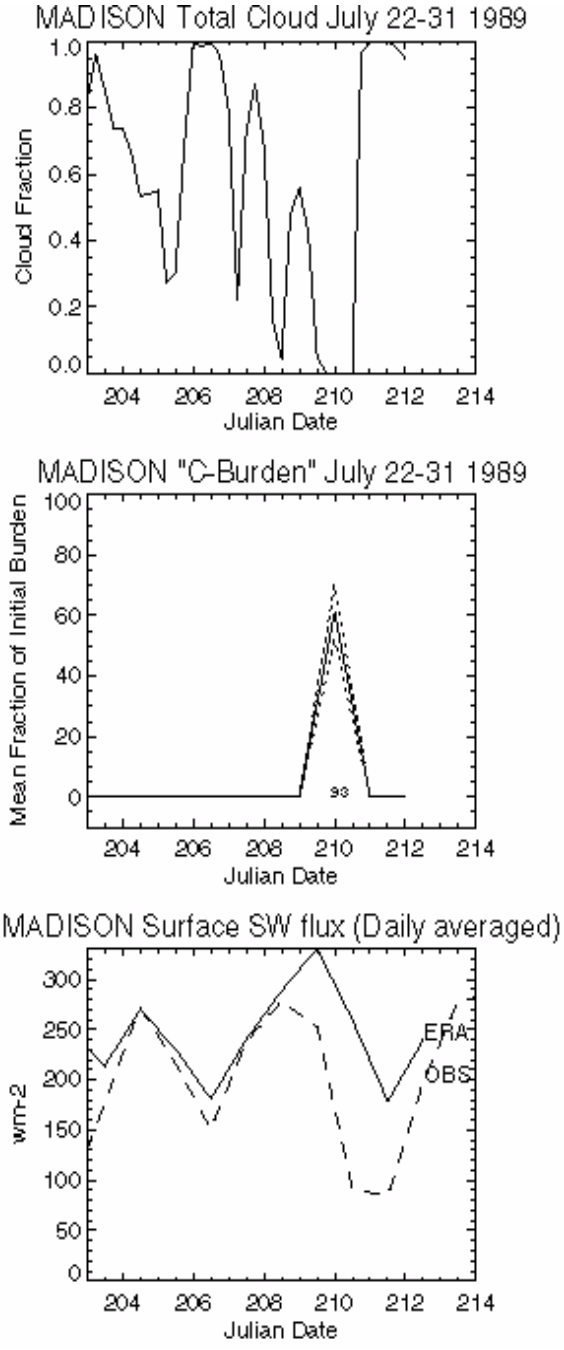

Figure 2: The 3-hourly cloud fraction from ERA-15 (top), the predicted aerosol amount (with # of parcels given) using the LTM and ERA-15 (middle) and the observed and ERA-15 predicted daily averaged solar insolation (W m^{-2}) (bottom) for Madison Wisconsin, USA, from July 22-31, 1989. Differences between the ERA-15 and observed solar insolation exceed 80 W m^{-2} during the period when smoke aerosol from the July 23 Manitoba

6. SUMMARY AND CONCLUSIONS

In this paper, we have introduced a method of inferring the radiative effect of smoke aerosols using a technique that combines satellite remote sensing with trajectory modeling. The results shown here clearly show large flux biases between theoretical and measured radiative fluxes correlate with the arrival of smoke aerosol to the area. Further analysis is required to convincingly demonstrate that the reason for these differences is the radiative effect of the smoke aerosols. To do this, the estimated fluxes taken from the ERA-15 will be recomputed every 3 hours using International Satellite Cloud Climatology Project (ISCCP) data set entitled "DX" gridded to a 1^{o} equal angle resolution (see paper 7B.2 for details). Surface radiometric and ancillary data for several more Canadian surface sites are being obtained at minute temporal resolution. The ultimate purpose of this research is to derive aerosol smoke maps for fire events such as this to be included in an aerosol climatology and be incorporated in the computation of the earth's surface radiation budget to better understand the radiative effect of aerosols.

ACKNOWLEDGEMENTS: Funding for this research was obtained through NASA headquarters under GACP and we gratefully recognize Robert Curran for facilitating the project.

7. REFERENCES

Baum, B. A., and Q. Trepte, 1999: A grouped threshold approach for scene identification in AVHRR Imagery. *J. Atmos. and Ocean. Tech* (in press).

Fairlie, T. D., R. B. Pierce, W. L. Grose, G. Lingenfelser, M. Loewenstein, and J. R. Podolske, 1997: Lagrangian Forecasting During ASHOE: Analysis of Predictive Skill for Analyzed and Reverse-Domain-Filled Potential Vorticity, *J. Geophys. Res.*, 102, 13,169-13,182

Hirsch, K.G., 1991: A chronological overview of the 1989 fire season in Manitoba. *The Forestry Chronicle*, **67**, 358-365.

Kaufman, Y.J., C. J. Tucker, and I. Fung, 1990: Remote sensing of biomass burning in the tropics. *J. Geophys. Res.*, **95**, 9927-9939.

Matson, M. G. Stephens, and J. Robinson, 1987: Fire detection using data from the NOAA-N satellites. *Int. J. Remote Sens.*, **8**, 961-970.

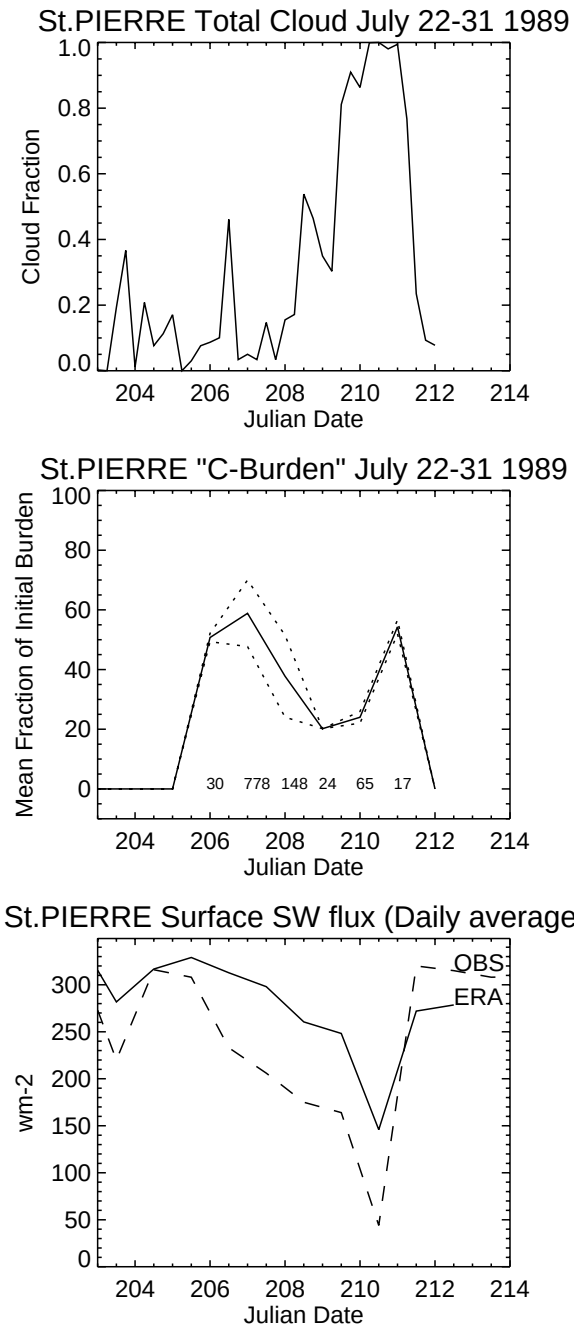

Figure 3: Same as Figure 2 except for St. Pierre and Miquelon, France, located just south of the island of New Foundland. Differences exceed 80 W m^{-2} during the period of the predicted smoke advection over the area.

Pierce, R. B., J-U Grooss, W. L. Grose, J. M. Russell III, P. J. Crutzen, T. D. Fairlie, G. Lingenfelser, 1997: Photochemical Calculations Along Airmass Trajectories During ASHOE/MAESA, *J. Geophys. Res.*, **102**, 13,153-13,167.